Modeling Trichloroethylene Degradation by a Recombinant Pseudomonad Expressing Toluene *ortho*-Monooxygenase in a Fixed-Film Bioreactor

Adam K. Sun, Juan Hong, Thomas K. Wood

Department of Chemical and Biochemical Engineering, University of California, Irvine, Irvine, California 92697-2575; telephone: 714-824-3147; fax: 714-824-2541; e-mail: tkwood@uci,edu

Received 18 July 1997; accepted 6 November 1997

Abstract: *Burkholderia cepacia* $PR1_{23}(TOM_{23C})$, expressing constitutively the TCE-degrading enzyme toluene *ortho*-monooxygenase (Tom), was immobilized on SIRAN™ glass beads in a biofilter for the degradation and mineralization of gas-phase trichloroethylene (TCE). To interpret the experimental results, a mathematical model has been developed which includes axial dispersion, convection, film mass-transfer, and biodegradation coupled with deactivation of the TCE-degrading enzyme. Parameters used for numerical simulation were determined from either independent experiments or values reported in the literature. The model was compared with the experimental data, and there was good agreement between the predicted and measured TCE breakthrough curves. The simulations indicated that TCE degradation in the biofilter was not limited by mass transfer of TCE or oxygen from the gas phase to the liquid/biofilm phase (biodegradation limits), and predicts that improving the specific TCE degradation rates of bacteria will not significantly enhance long-term biofilter performance. The most important factors for prolonging the performance of biofilter are increasing the amount of active biomass and the transformation capacity (enhancing resistance to TCE metabolism). © 1998 John Wiley & Sons, Inc. *Biotechnol Bioeng* **59:** 40–51, 1998.

Keywords: fixed-film bioreactor; biofilter model; trichloroethylene degradation

INTRODUCTION

Various reactor designs have been studied for biological treatment of numerous pollutants (Dikshitulu et al., 1993; Fan et al., 1990; Wang et al., 1996; Zilli et al., 1993), and mathematical models have been used successfully for further understanding these reactor designs. However, most of these pollutants can be utilized by the bacteria as the sole carbon and energy source for growth. Some volatile chlorinated aliphatic compounds can only be degraded through a cometabolic pathway, and trichloroethylene (TCE) has been used as the model pollutant (Coyle et al., 1993; Folsom and Chapman, 1991; Lackey et al., 1993; Phelps et al., 1990; Taylor et al., 1993; Wilcox et al., 1995). The most commonly studied microorganisms for TCE degradation are *Methylosinus trichosporium* OB3b (McFarland et al., 1992; Oldenhuis et al., 1989; Strand et al., 1991) and *Burkholderia cepacia* G4 (formerly *Pseudomonas cepacia* G4) (Ensley and Kurisko, 1994; Folsom and Chapman, 1991; Landa et al., 1994; Nelson et al., 1986; Shields et al., 1991).

A fixed-film bioreactor with large amounts of biomass can be an attractive reactor for remediating organic wastes (Hao et al., 1991; Kirchner et al., 1992; Shareefdeen et al., 1993). Gas containing volatile organic compounds, such as TCE, is passed through the supporting matrix, and the immobilized bacteria degrade the organic compounds. Because fixed-film bioreactors can treat the contaminant in the gas phase in a contained environment, introduction of TCE-degrading organisms (either wild-type or genetically-engineered microorganisms) into the environment is minimized, and indigenous microorganisms from the polluted sites may be filtered from the incoming gas to avoid contamination (Ensley and Kurisko, 1994). Even though biofilters have been used widely for various industrial wastes, data available for improving performance are limited (Hodge and Devinny, 1995). To understand reactor operation, a pure culture should provide a simpler system than a consortium of microorganisms.

The greatest advantage of *Burkholderia cepacia* $PR1_{23}(TOM_{23C})$ (henceforth $PR1_{23}$) is its ability to constitutively express toluene *ortho*-monooxygenase (Tom), which is responsible for TCE degradation (Shields and Reagin, 1992; Shields et al., 1994). Because $PR1_{23}$ does not require an inducer (such as methane or toluene), it is an excellent microorganism for TCE bioremediation (no competitive inhibition). In addition, $PR1_{23}$ has high growth rates and high TCE degradation and mineralization rates in various media (Sun and Wood, 1996); thus, $PR1_{23}$ was selected

Correspondence to: Thomas Wood

Contract grant sponsors: California EPA Department of Toxic Substances Control; Army Research Office; Fluor Daniel, Inc.

Contract grant numbers: 93-T0527; DAAL 03-92-0398

CCC 0006-3592/98/010040-12

for use in an aerobic, single-pass, fixed-film bioreactor, which was shown to be feasible for degrading and mineralizing gas-phase TCE (Sun and Wood, 1997). However, due to formation of toxic TCE breakdown products (Wackett and Gibson, 1988; Zylstra et al., 1989), the performance of $PR1_{23}$ biofilter deteriorated with continuous TCE addition, and the extent of TCE degradation ability decreased faster with higher TCE concentration (Sun and Wood, 1997).

One of the most important parameters governing fixed-film reactor performance is the mass transfer resistance from the gas phase to the liquid phase which can be the rate-limiting step (Karel et al., 1985) for TCE degradation. Also, cells have been shown to change upon immobilization (e.g., enzyme productivity, long-term stability, nutrient uptake, and cellular growth rates) (Hao et al., 1991; Karel et al., 1985). The activity of TCE-degrading enzyme in the biofilm may be lower than that of suspended cells under similar growth conditions, and TCE transport through the cells in the biofilter might be altered. The objective of this study was to develop a mathematical model to predict the performance of the $PR1_{23}$ fixed-film bioreactor in the absence of adsorption (using an inert matrix) and to investigate the parameters which effect its performance.

There are numerous biofilter models for the degradation of volatile organic chemicals, and these models can be classified into two groups: those in which the volatile organic chemicals can be degraded either as a sole carbon and energy source and those in which the pollutant is degraded by a fortuitous pathway (e.g., TCE). When ethanol is used as a carbon and energy source, Hodge and Devinny (1995) developed a model describing a biofilter with adsorption using first-order kinetics, and the ethanol-laden air was introduced to the biofilter without continuous addition of liquid nutrient (no material balance in the biofilm/liquid phase). Utgikar et al. (1991) proposed a model for the biodegradation of volatile organic compounds in a biofilter where the substrate was used as the carbon and energy source (e.g., toluene); they partitioned the biofilter system into four distinct sections (gas phase, liquid phase, biofilm, and packing material), and the model included terms describing mass transfer by diffusion, biomass growth, and constant biomass decay (constant coefficient for decay rate). First-order biodegradation was used by simplifying the Monod kinetics with the assumption that the substrate concentration is much lower than the half-saturation constant (or Michaelis constant); however, no experimental data were presented to verify the model. The model derived by Shareefdeen et al. (1993) described and predicted experimental results for the biofiltration of methanol vapor, which served as the carbon source for the bacteria growth. No liquid nutrient was used in this study, and the assumption of steady state or quasi-steady state was used for obtaining a numerical solution. This model did not include convection phenomena (only diffusion), and the amount of biofilm was not quantified.

To describe fortuitous degradation of TCE, Duncan et al. (1995) developed a two-phase model utilizing convective mass transfer from the liquid phase to the biofilm for describing TCE stripped from the liquid by gas as well as the biological degradation of TCE; deactivation of the enzyme was not included. This model was consistent with limited experimental data. Hecht et al. (1995) used a bubble-column bioscrubber for cometabolic degradation of TCE, and the model was based on plug flow for the gas phase and pseudo-first-order kinetics for TCE degradation. At the experimental conditions evaluated by Hecht et al., TCE degradation was limited by the reaction rate (not mass transfer limited). Hecht et al., suggested the best way to increase TCE degradation in the bioscrubber was to use a microorganism with high degradation rates. A mathematical model was also developed for dechlorination of TCE in a hollow-fiber membrane biofilter (Parvatiyar et al., 1996) under steady-state conditions, and the dechlorination of TCE occurred in the anaerobic zone of the biofilm. The model proposed in this article differs from the models cited previously by including axial dispersion, a material balance in both the gas and the liquid phase, and Monod kinetics for biodegradation coupled with deactivation of the TCE-degrading enzyme. To our knowledge, this is the first model developed for TCE degradation using a fixed-film bioreactor and verified with experimental data.

MATHEMATICAL MODEL

The basic axial dispersion-convection model was used as the core (Wankat, 1990), and the mass transfer and biodegradation terms were incorporated into this model. The following assumptions were made to simplify the model: (1) the biofilter consists of a three-phase system: air, liquid/biofilm, and solid, inert, non-porous carriers (bacteria inside the porous carrier were neglected); (2) solid carriers are homogenous in size (0.30 cm in diameter) with a uniform liquid/biofilm thickness around the carriers; (3) the liquid/biofilm phase is homogenous without a boundary separating the liquid and the biofilm; (4) the average biomass measured at the end of the experiment represents the total biomass that was distributed evenly and was relatively constant during the experiment; (5) the liquid-phase concentration of TCE at the gas/liquid interface is at equilibrium with the bulk gas-phase TCE concentration ($C^*_{l,TCE} = C_{g,TCE}/H_{TCE}$, where H_{TCE} is the Henry's law constant).

Because oxygen is required for biofilm formation and TCE degradation, lack of sufficient oxygen in the biofilm can limit TCE degradation. Thus, the biodegradation rate of TCE by $PR1_{23}$ was expressed in terms of both TCE and oxygen concentrations using the dual-substrate Monod equation for TCE (Bailey and Ollis, 1986; Chang and Alvarez-Cohen, 1995). Exposure to TCE has been shown to deactivate cellular proteins via the toxic metabolites derived from TCE metabolism (Oldenhuis et al., 1991; Wackett and Gibson, 1988; Wackett and Householder, 1989; Zylstra et al., 1989); therefore, the biomass responsible for TCE deg-

radation was assumed to deactivate at a rate proportional to the rate of TCE degradation (Alvarez-Cohen and McCarty, 1991; Chang and Alvarez-Cohen, 1995; Chu and Alvarez-Cohen, 1996).

As the TCE-laden air passes through the fixed-film bioreactor (Fig. 1), its concentration can be affected by axial dispersion, convection, mass transfer, and biodegradation. Based on the above assumptions, an unsteady-state model was obtained with the determination equations by making a mass balance on TCE and oxygen in the gas (θ is the fractional gas phase volume) and liquid/biofilm phase (ε is the fractional liquid-phase volume):

$$\frac{\partial C_{g,TCE}}{\partial t} = D_{g,TCE}\frac{\partial^2 C_{g,TCE}}{\partial x^2} - \frac{Q_A}{\theta A}\frac{\partial C_{g,TCE}}{\partial x} - \frac{K_{L,TCE}a}{\theta}(C^*_{l,TCE} - C_{l,TCE}) \quad (1)$$

$$\frac{\partial C_{g,O2}}{\partial t} = D_{g,O2}\frac{\partial^2 C_{g,O2}}{\partial x^2} - \frac{Q_A}{\theta A}\frac{\partial C_{g,O2}}{\partial x} - \frac{K_{L,O2}a}{\theta}(C^*_{l,O2} - C_{l,O2}) \quad (2)$$

$$\frac{\partial C_{I,TCE}}{\partial t} = D_{l,TCE}\frac{\partial^2 C_{l,TCE}}{\partial x^2} - \frac{Q_l}{\varepsilon A}\frac{\partial C_{l,TCE}}{\partial x} + \frac{K_{L,TCE}a}{\varepsilon}(C^*_{l,TCE} - C_{l,TCE}) - V_{max}X\frac{C_{l,TCE}}{K_{M,TCE} + C_{l,TCE}}\frac{C_{l,O2}}{K_{M,O2} + C_{l,O2}} \quad (3)$$

$$\frac{\partial C_{l,O2}}{\partial t} = D_{l,O2}\frac{\partial^2 C_{l,O2}}{\partial x^2} - \frac{Q_l}{\varepsilon A}\frac{\partial C_{l,O2}}{\partial x} + \frac{K_{L,O2}a}{\varepsilon}(C^*_{l,O2} - C_{l,O2}) - V_{max}XY_{O2}\frac{C_{l,TCE}}{K_{M,TCE} + C_{l,TCE}}\frac{C_{l,O2}}{K_{M,O2} + C_{l,O2}} - Y_{resp}X \quad (4)$$

$$\frac{dX}{dt} = -\frac{1}{T_C}\frac{V_{max}XC_{l,TCE}}{K_{M,TCE} + C_{l,TCE}}\frac{C_{l,O2}}{K_{M,O2} + C_{l,O2}} \quad (5)$$

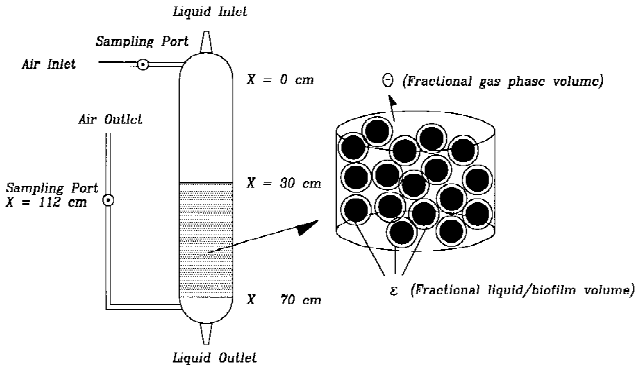

Figure 1. Schematic of the fixed-film bioreactor (dead spaces shown).

Equations (1) and (2) describe the mass balance of TCE and oxygen in the gas phase (using axial dispersion, convection, and mass-transfer terms). Equations (3) and (4) describe the mass balance of TCE and oxygen in liquid/biofilm phase. The second term on the right side of Equations (3) and (4) describes the liquid medium flowing around the carriers (upon which a biofilm has formed). The last term in Equation (4) characterizes the background oxygen consumption by the biofilm (respiration) that is not associated with TCE degradation (Bailey and Ollis, 1986). Equation (5) describes the decrease in active biomass available for TCE degradation due to toxic TCE breakdown products.

The initial and boundary conditions required to solve these equations are

$$t = 0 \quad C_{g,TCE} = C_{g,TCE,inlet} \quad C_{g,O2} = C_{g,O2,inlet} \quad (6)$$

$$C_{l,TCE} = 0 \quad C_{l,O2} = C_{l,O2,initial} \quad (7)$$

$$X = X_{initial} \quad (8)$$

$$x = 0 \quad C_{g,TCE} = C_{g,TCE,inlet} \quad (9)$$

$$C_{g,O2} = C_{g,O2,inlet} \quad (10)$$

$$C_{l,TCE} = 0 \quad (11)$$

$$C_{l,O2} = 0 \quad (12)$$

$$x = L \quad \frac{\partial C_{g,TCE}}{\partial x} = 0 \quad \frac{\partial C_{g,O2}}{\partial x} = 0 \quad (13)$$

$$\partial Cl,TCE\partial x = 0 \quad \partial Cl,O2\partial x = 0 \quad (14)$$

These equations were solved using a numerical simulation (IMSL MOLCH subroutine using the method of lines, Visual Numerics, Inc., Houston, TX) with parameter input values listed in Table I. Due to the reactor design, there are dead spaces before and after packing in the fixed-film bioreactor (Fig. 1). To predict the TCE breakthrough curve, these dead spaces were included in the numerical simulation.

EXPERIMENTAL APPROACH

The biofilter and experimental procedures have been described previously (Sun and Wood, 1997). *Burkholderia cepacia* G4 (henceforth G4) is the parent strain of *Burkholderia cepacia* $PR1_{23}(TOM_{23C})$ and expresses Tom only in the absence of glucose and in the presence of phenol or toluene; hence, G4 was used as the negative control (biotic) for this study. G4 and $PR1_{23}$ were cultivated in a 0.4 w/v % glucose chloride-free minimal medium (with 50 μg/mL of kanamycin for $PR1_{23}$). The supporting material used in this

Table I. Parameters for the packed portion of the fixed-film bioreactor (x = 30 to 70 cm).

Parameter	Value	Units
A	17.7	cm^2
$D_{g,O2}$	7.45	cm^2/min
$D_{g,TCE}$	7.45	cm^2/min
$D_{l,O2}$	0.296	cm^2/min
$D_{l,TCE}$	0.296	cm^2/min
H_{O2}	34.9	—
H_{TCE}	0.4	— (Folsom et al., 1990)
$K_{L,O2}a$	242.5	1/min
$K_{L,TCE}a$	242.5	1/min
$K_{M,O2}$	0.048	mg O_2/L
$K_{M,TCE}$	35.0	mg TCE/L
L	70	cm
Q_A	0.100	L/min
Q_l	0.000694	L/min
T_C	0.065–0.204	mg TCE/mg protein (Table III)
V_{max}	0.00237	mg TCE/min/mg protein (Sun and Wood, 1996)
Y_{O2}	0.49	mg O_2/mg TCE
Y_{resp}	0.001	mg O_2/min/mg protein
X	4.2–18	g protein/mL liquid
ε_b	0.5	cm^3 void volume/cm^3 reactor
ε	0.18	cm^3 liquid/cm^3 reactor
θ	0.32	cm^3 of gas/cm^3 of reactor

study for biofilm attachment and growth (surface-attached process) was open-pore sintered glass (SIRAN™ carriers) with particle size 2 to 5 mm and 60–300 μm internal pores (Jaeger Biotech Engineering, Inc., Costa Mesa, CA).

Confocal Scanning Laser Microscopy (CSLM)

SIRAN™ carriers with biofilm were removed from the biofilter (after 10 d of biofilm formation) from four different segments, and the biofilms were stained for 30 min using the Live/Dead *Bac*lit bacterial viability assay kit (Molecular Probes, Eugene, OR). The assay distinguishes the live and dead cells based on the membrane integrity. Using the confocal scanning laser microscope equipped with a krypton/argon laser (MRC 1024, Bio-Rad, Hercules, CA), the biofilms were excited at 488 nm, and the fluorescent light was visualized using a T1/E2 multi-purpose filter combination; the live cells fluoresce green and the dead cells fluoresce red. Thin vertical sections (1 μm) of biofilm image were collected, and the images were analyzed for fraction of live and dead cells based on different pixel intensities of live and dead cells. The images were analyzed using the COMOS software on the BioRad MRC600.

Independent Parameter Determination

Characterization of the Biofilms (Table I)

$PR1_{23}$ biofilms on SIRAN™ carriers were visualized by CSLM, and the images of the biofilm at different segments of the biofilter were collected to characterize the biofilms. The cell density was higher for the biofilm near the top of the biofilter (near the nutrient inlet), and the biofilm cell density decreased slightly (~10 to 30% based on visual analysis) as axial distance increased. The fractions of live and dead cells were relatively uniform along the biofilter axial position (six images each from four different axial sections were analyzed and averaged 49.5% ± 20.3 live vs. 50.4% ± 20.3 dead cells, Table II). The fraction of live and dead cells along the biofilm thickness (near the nutrient inlet) was also analyzed. The proportions of live and dead cells were relatively uniform along the biofilm thickness, and this profile was consistent at each position in the axial direction (data not shown).

The biofilm thickness on SIRAN™ carriers was determined by three methods. For the CSLM analysis, the SIRAN™ beads were placed on microscope slides using an inverted stage; hence, the images were obtained as the biofilms were compressed against the microscope slides due to the weight of the beads. Thus, the measured biofilm using CSLM (30 to 80 μm) underestimates the actual biofilm thickness. The average biofilm thickness was also calculated based upon the total amount protein measured at the end of each biofilter experiment. Based on the size of rod-shaped *Pseudomonas* (0.75 × 3.25 μm) (Singleton and Sainsbury, 1988), an average volume of 5.74×10^{-12} cm^3/cell is calculated. Assuming 50% void space in the biofilm (de Beer et al., 1994), the biofilm thickness was estimated as 41 to 230 μm with a conversion factor of 48.08 mg protein/cm^3 of biofilm (Sun and Wood, 1996). The third method used to estimate the biofilm thickness was based on liquid holdup volume in the biofilter. Using a 500-mL biofilter (50% void space) and after ten days of biofilm formation, the biofilter was filled completely with liquid medium. By carefully draining the liquid to minimize biofilm sloughing, 160 mL of liquid was collected. Assuming the biofilm volume represents the liquid holdup in the biofilter, the total biofilm volume was 90 mL [500 mL reactor volume × 0.5 (void) − 160 mL (liquid-drained volume)]. With an average bead diameter of 0.3 cm (approximately 17,693 beads in 500-mL reactor), the estimated liquid holdup volume per bead was 5.09×10^{-3} cm^3, which represents 162 μm of biofilm thickness.

Table II. Characterization of the *Burkholderia cepacia* $PR1_{23}$ (TOM_{23c}) biofilm by CSLM after 10 d of growth. Number of experiments indicated by n.

Respective axial position in the biofilter	Biofilm thickness (δ) μm	Live: dead cells (number of images)
Top	70 ~ 80	67 : 33 (n = 3)
1/3 from the top	45 ~ 50	23 : 77 (n = 1)
2/3 from top	50 ~ 60	45 : 55 (n = 1)
Bottom	30 ~ 35	63 : 37 (n = 1)

Kinetics of TCE and Oxygen Metabolism

The Monod kinetic parameters for TCE degradation by $PR1_{23}$ were determined using shake flask experiments (V_{max} = 0.00237 mg TCE/min/mg protein and $K_{M,TCE}$ = 3.81 mg TCE/L) (Sun and Wood, 1996). Because aerobic bacteria require oxygen for their metabolism, the affinity for oxygen ($1/K_{M,O2}$) should be much higher than TCE, even in a biofilm environment. It has been estimated that for a pure culture of *Pseudomonas putida* biofilm grown on phenol, the Michaelis constant for oxygen ($K_{M,O2}$) is 0.048 mg O_2/L (Beyenal et al., 1997).

Overall Mass Transfer Coefficient

Using the Thoenes-Kramers mass transfer correlation for flow-through packed beds (Fogler, 1992), $Sh' = 1.0\ (Re')^{1/2}Sc^{1/3}$, the overall mass transfer coefficient for oxygen ($K_{L,O2}$) was calculated as 19.75 cm/min. The parameter a (interfacial area of gas/liquid per a unit of reactor volume) was estimated (Westerterp et al., 1984) by calculating the total surface area of SIRAN™ beads and divided by the total reactor volume (a = 12.28 cm^2 of area/cm^3 of reactor). Thus, the overall volumetric liquid mass transfer coefficients for oxygen ($K_{L,O2}a$) was 242.5 1/min. This same value was used for $K_{L,TCE}a$.

Henry's Law Constants

A dimensionless Henry's law constant of 0.4 was used for TCE (Folsom et al., 1990). The Henry's law constant for oxygen at 30°C was calculated as 272 mg/L/7.8 mg/L = 34.9. The oxygen concentration of TCE-laden air was also taken as 272 mg/L for all cases.

Yield Coefficient (Y_{O2}) and Background Respiration Coefficient (Y_{resp})

Overall TCE mineralization by aerobic microorganisms requires two moles of oxygen for every mole of TCE (Alvarez-Cohen and McCarty, 1991; McFarland et al., 1992):

$$C_2HCl_3 + NADH + H^+ + 2O_2 \rightarrow 2CO_2 + NAD^+ + 3HCl \quad (15)$$

Hence, Y_{O2} coefficient for TCE degradation was calculated as 0.49 mg O_2/mg TCE. Previously, effluent $PR1_{23}$ cells were collected and background oxygen consumption rates were measured using a biological oxygen monitor (Sun and Wood, 1997). The background oxygen consumption rate (Y_{resp}) was approximately 0.001 mg O_2/min/mg protein, and this value was used in the model. This value compares well with the calculated values (0.0002 to 0.0009 mg O_2/min/mg protein) using the yield factor relating grams of cells formed per gram of O_2 consumed ($Y_{X/O2}$ of 0.20 to 0.85 g cell/g O_2 for *Pseudomonas*, Bailey and Ollis, 1986), and the estimated growth rate of $PR1_{23}$ in the biofilter (μ_{max} = 0.0052/h, based on biomass data in Table III).

Table III. Biomass levels of the $PR1_{23}$ biofilter with 0.7 L of SIRAN™ matrix and an air flow rate of 0.1 L/min.

TCE conc. (mg/L of air)	Average biomass conc. (mg protein from live cells/mL of liquid)[a]	T_C (g TCE/g live protein)[b]	Length of experiment (days)
0.040	18.0 ± 11.6	0.071	22
0.242	4.2 ± 2.5	0.107	10
	8.3 ± 4.3	0.065	24
1.210	4.4 ± 2.5	0.204	11
2.420	8.1 ± 6.2	0.129	7

[a]Average biomass concentration involved in TCE degradation [(g average protein measured/mL reactor) * fraction of live cells/ε (mL of liquid/mL reactor)].

[b]T_C (g of TCE degraded per g of protein from live cells involved in TCE degradation) [(g TCE/g total protein)/fraction of live cells].

Biomass Concentration

If the actual biofilm concentration in the biofilter was known, assumption (4) that the biomass at the end of the experiment was constant would not be necessary. However, due to the construction of the reactor, the biomass concentration was measured only at the end of each experiment (measuring biomass during the experiment could contaminate the biofilter). The total protein concentrations measured (protein from the live and dead cells) at the end of each experiment do not necessarily represent the amount of protein at the beginning of the experiment, and the total protein concentration measured at the end of the experiment could be much higher than the initial protein concentration (the biofilm was visible after 2 to 3 d of culturing, the biomass concentration was most robust at the top of biofilter near the nutrient inlet, and the biofilm at the bottom of biofilter was only visible after approximately three to seven days). As indicated in the biofilm characterization using CSLM, the fraction of live cells in the biofilm was approximately 50%. Thus, the actual amount of cells which were potentially involved in TCE degradation would be half the measured protein concentration. As shown in Table III, there seems to be little correlation between the biomass concentration and the length of experiment or the TCE concentrations.

Transformation Capacity (T_C)

As reported earlier (Sun and Wood, 1997), $PR1_{23}$ which lost active Tom failed to regain its ability to express the TCE-degrading enzyme constitutively. Thus, even with new $PR1_{23}$ biofilm growth in the biofilter (absence of contaminants verified by daily plating of the biofilter effluent and by a colony lift with a *tom* probe), no new TCE-degrading enzyme was expressed after Tom activity was completely

lost. Hence, the model does not incorporate cell growth terms.

To take into account that TCE degradation kills cells, the transformation capacity was used to reduce the amount of active biomass. Transformation capacity is the maximum amount of cometabolized TCE that can be degraded per unit mass of resting cells (Alvarez-Cohen and McCarty, 1991). Assuming complete TCE breakthrough occurs when the TCE-degrading enzyme is completely deactivated, and the biofilm distribution in the bioreactor does not change significantly, the transformation capacity (T_C) was determined by dividing total amount of TCE degraded by the total amount of biomass in the reactor. From the five TCE breakthrough curves [0.04, 0.242 (two experiments), 1.21, and 2.42 mg TCE/L], $PR1_{23}$ oxidized approximately an average of 0.058 ± 0.033 mg of TCE per mg of total protein before Tom activity was completely inactivated. The biomass varied from 4.2 to 18.0 g of protein/mL of liquid, and this large difference in biomass concentration resulted in a range of T_C values. Due to this large difference in T_C values, the individual T_C and the average T_C were used in the model and compared with the experimental data. The simulations with the individual T_C from each of the experimental results agreed better than the simulations which used the average T_C value. Thus, the specific T_C value measured for each experiment was used. Because ~50% of the protein is from dead cells (CSLM results, Table II), the T_C values were corrected accordingly.

Relative Liquid (ε) and Gas Volume (θ)

Assuming the liquid holdup represents biofilm volume in the biofilter, the fraction of liquid phase (ε) in the biofilter was 0.18 (90 mL/500 mL), and the fraction of gas phase (θ) in the biofilter was 0.32 [1.0 – 0.5 (beads) − 0.18 (ε)]. These values were used for all simulations.

Estimation of Parameters Using Experimental Data

Michaelis Constant ($K_{M,TCE}$) for TCE Degradation (Figure 2)

Using the Michaelis constant ($K_{M,TCE}$ = 3.81 mg/L) determined from shake-flask experiments (Sun and Wood, 1996), entirely different TCE breakthrough profiles were obtained as compared to the experimental data. Hence, $K_{M,TCE}$ in the biofilm was estimated using the experimental data of the $PR1_{23}$ biofilter at 2.42 mg/L TCE concentration based on curve fitting the model with the experimental data ($K_{M,TCE}$ = 35 mg TCE/L). This new $K_{M,TCE}$ value was used along with the shake flask-determined V_{max} to predict the TCE breakthrough curves for the other TCE concentrations. Because the Michaelis constant used in this model represents both the inverse of the affinity of the intact cells for the substrate and substrate diffusion through the cellular membrane and biofilm, it can be influenced by the biofilm where dead cells and exopolysaccharide may dominate (Jayaraman et al., 1997). Hence, it is reasonable the affinity of the live cells for the substrate could decrease significantly compared to suspended cells and a higher Michaelis constant for TCE is reasonable.

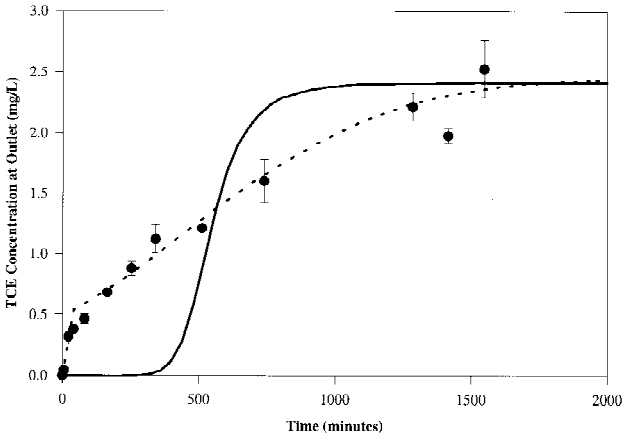

Figure 2. TCE breakthrough curve of the $PR1_{23}$ biofilter at 2.42 mg TCE/L of air (used to determine $K_{M,TCE}$ of the biofilter). Filled circle (●) represents experimental data (standard deviation shown), solid line (—) represents model prediction with $K_{M,TCE}$ = 3.81 mg/L (shake-flask parameter), and dotted line (····) represents model fit with $K_{M,TCE}$ = 35 mg/L.

Axial Dispersion Coefficients

To obtain the axial dispersion coefficient for TCE in the gas phase ($D_{g,TCE}$), three experiments were performed using a 1.1 L reactor packed with dried SIRAN™ carriers (reactor length = 62.5 cm, interstitial air velocity = 3.125 cm/min). The dead spaces before and after the reactor were removed. Using TCE as the pulse-tracer, $D_{g,TCE}$ was calculated to be approximately 7.45 cm^2/min by fitting the experimental data with the analytical solution for the axial dispersion model (Mysliwiec et al., presented at the Air & Waste Management Association Meeting, Nashville, TN, June 1996), $C_{g,TCE}) = 1/\sqrt{4\pi D_{g,TCE}}\ \exp\{-(x - vt)^2/4D_{g,TCE}t\}$ (data not shown), and this same value was used for $D_{g,O2}$. Due to significant broadening of the TCE tracer concentration, the axial dispersion in the gas phase cannot be ignored. The axial dispersion coefficient in the liquid phase ($D_{l,TCE}$) was calculated based on a correlation used for a two-phase packed bed (0.296 cm^2/min) (Mak et al., 1991). This same value was used for $D_{l,O2}$.

RESULTS AND DISCUSSION

Verification of the Biofilm Model

To validate the mathematical model, numerical simulations of TCE breakthrough curves for the abiotic (no cells) and

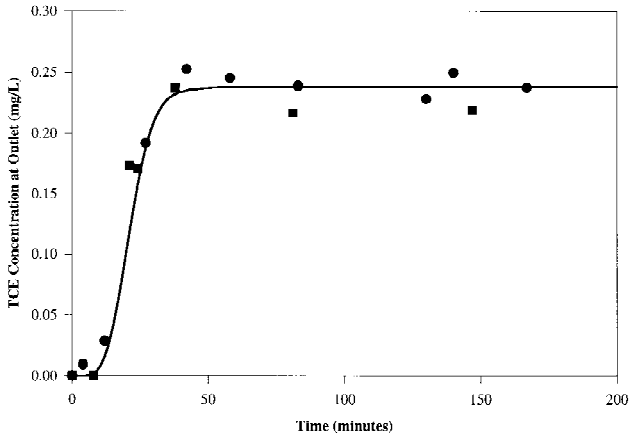

Figure 3. TCE breakthrough curves of abiotic (no cells) and biotic (wild-type *B. cepacia* G4 grown on glucose and without induction of the Tom enzyme) controls. Filled circle (●) represents abiotic control, filled square (■) represents biotic control, and solid line (—) represents model prediction for abiotic and biotic controls.

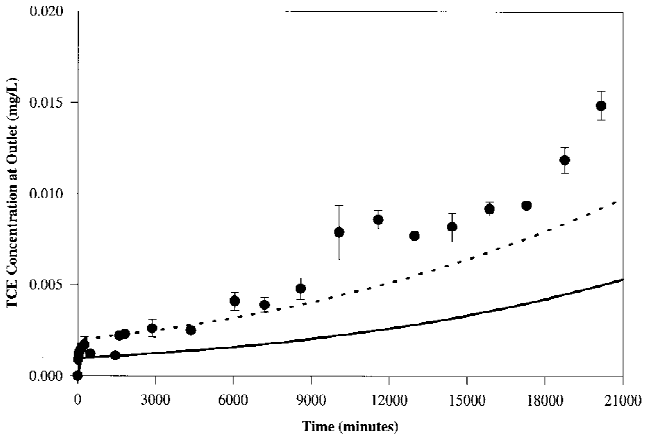

Figure 4. TCE breakthrough curve of $PR1_{23}$ biofilter at 0.04 mg TCE/L of air. Filled circle (●) represents experimental data (standard deviation shown), solid line (—) represents model prediction, and dotted line (· · · ·) represents model prediction with corrected biomass (20% less than the measured).

biotic (G4 cells without TCE-degrading enzyme expressed) control experiments were performed at a TCE concentration of 0.242 mg/L in air at 0.1 L/min air (Fig. 3). Using the parameter values listed in Table III, the model predicted the breakthrough time of 39 min (95% of inlet TCE concentration seen at the outlet) for the abiotic and biotic biofilters; experimental data for the breakthrough of the abiotic and biotic biofilter was achieved in approximately 40 min after TCE addition for both controls. If the axial dispersion terms in the gas phase and the liquid phase were deleted, the model predicts the breakthrough time of 26 min. Thus, the axial dispersion terms are significant and should not be ignored.

The numerical output of TCE concentration in both the gas and liquid phases were totaled to verify the material balance for the abiotic and biotic control (no TCE degradation). At an inlet TCE concentration of 0.242 mg/L in air at 0.1 L/min air flow and 0.000694 L/min liquid flow, the outlet TCE concentration of 0.2379 mg/L in air and 0.5947 mg/L in liquid was obtained (which indicates equilibrium was reached for the gas and liquid TCE concentrations, i.e., $H = 0.4$). The inlet and outlet TCE mass flow rates are nearly identical. The material balance for the TCE shows that less than 2% of the inlet TCE is removed from the gas phase (due to liquid adsorption) for the control simulations. A material balance on oxygen was also verified (data not shown).

TCE Breakthrough Curves Predicted by the Model

For simulations of TCE degradation at different TCE concentrations in the presence of Tom-expressing $PR1_{23}$, the measured biomass concentration and calculated transformation capacity for each experiment was used. Figures 4 to 8 (solid lines) show the model predictions compared to the experimental TCE concentration measured at the reactor exit (Sun and Wood, 1997). The model predicted the general trend of the TCE breakthrough profile with bioremediation; however, for $t < 1000$ min, higher biodegradation rates of TCE were achieved than the model predicted (~60 to 100% higher than model prediction, Figs. 5–7).

The most important parameter affecting the simulations was the biomass concentration. Because the biofilm was seeded by recirculating a concentrated inoculum culture (equivalent to 0.55 mg protein/mL culture) and developing the biofilm for 5 to 10 d with glucose medium (Sun and Wood, 1997), the actual biomass present for TCE degradation was less than the biofilm concentration measured at the end of the experiments. This increase in biofilm development over the course of the experiments was supported by visual observations. Therefore, by reducing by 20% the amount of live cells involved in TCE degradation measured

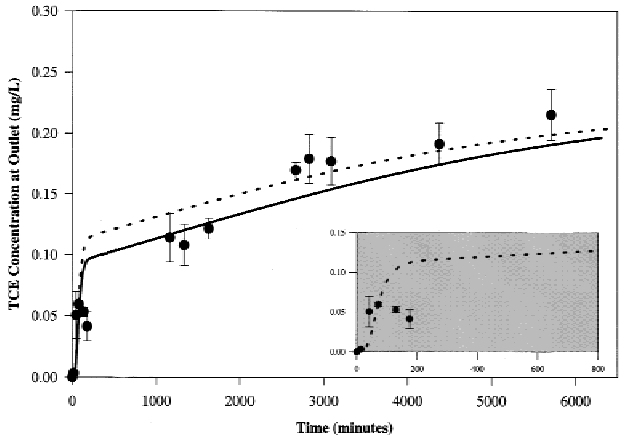

Figure 5. TCE breakthrough curve of $PR1_{23}$ biofilter at 0.242 mg TCE/L of air (experiment #1, low biomass of 4.2 ± 2.5 mg protein/mL liquid). Filled circle (●) represents experimental data (standard deviation shown), solid line (—) represents model prediction, and dotted line (· · · ·) represents model prediction with corrected biomass (20% less than the measured).

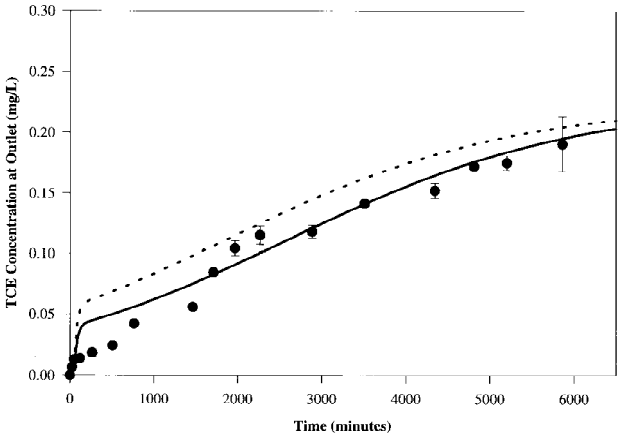

Figure 6. TCE breakthrough curve of $PR1_{23}$ biofilter at 0.242 mg TCE/L of air (experiment #2, high biomass of 8.3 ± 4.3 mg protein/mL liquid). Filled circle (●) represents experimental data (standard deviation shown), solid line (—) represents model prediction, and dotted line (· · · ·) represents model prediction with corrected biomass (20% less than the measured).

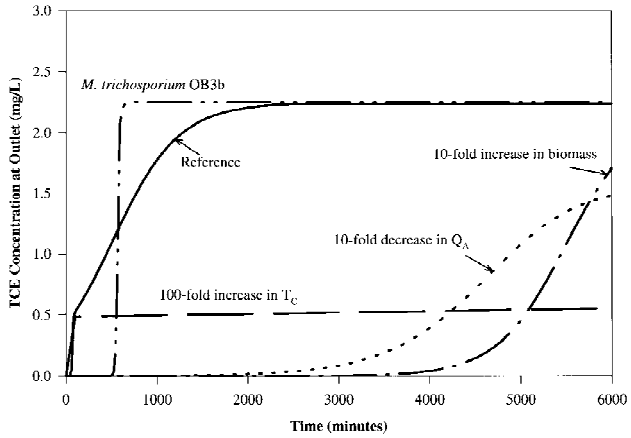

Figure 8. Predicted TCE breakthrough curves for *M. trichosporium* OB3b, higher T_C, lower Q_A, and higher biomass (2.42 mg TCE/L). Solid line (—) represents the reference model prediction (0.1 L/min air flow), dotted line (· · · ·) represents a 10-fold decrease in the volumetric air flow rate (Q_A), dashed-dotted-dotted line (– · · –) represents *M. trichosporium* OB3b (V_{max} = 0.067 mg TCE/min/mg protein and $K_{M,TCE}$ = 19 mg/L), long dashed line (– –) represents a 100-fold increase in T_c and dashed-dotted line (– · –)represents 10-fold increase in active biomass.

by the protein assay at the end of the experiment, better agreement was attained between the model and the experimental data at 0.04, 0.242 (experiment #1), and 1.21 mg/L TCE concentrations [Figs. 4, 5, and 7 (dotted lines), respectively]. Also, either non-uniform air flow through the biofilter (from channeling of air) or the presence of stagnant regions would cause less biomass to be exposed to TCE.

This importance of the biomass concentration is shown by the results from two identical experiments conducted at a TCE concentration of 0.242 mg/L (Figs. 5 and 6) in which there was a significant difference in the average biomass level measured at the end of each experiment (~2-fold difference, Table III). This large difference in average biomass level affected the biodegradation of TCE in the biofilter, because the TCE concentrations measured at the effluent of the biofilter were 0.11 mg/L and 0.04 mg/L after 1000 min of TCE addition for the lower biomass experiment (Fig. 5, biomass of 4.2 ± 2.5 mg protein/mL liquid) and higher biomass experiment (Fig. 5, biomass of 8.3 ± 4.3 mg protein/mL liquid), respectively.

At a high TCE concentration (2.42 mg/L of air), the TCE breakthrough time for the biofilter was faster than the lower TCE concentration (0.04 mg/L) due to inactivation of TCE-degrading enzyme caused by the TCE metabolites (50% breakthrough for 2.42 mg/L vs. only 5% breakthrough for 0.04 mg/L after 500 min of TCE addition). Thus, at lower TCE concentrations, the biofilter can be used for longer periods.

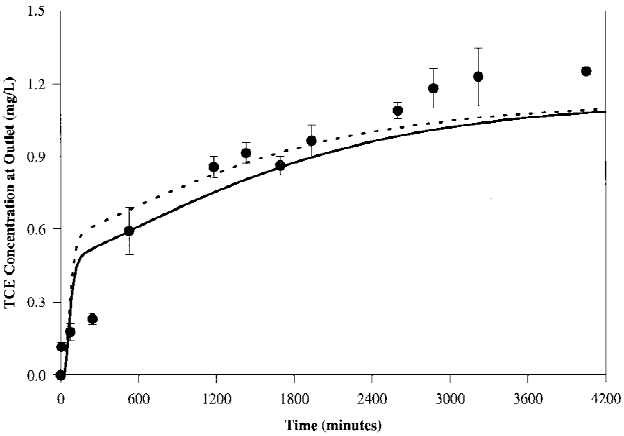

Figure 7. TCE breakthrough curve of $PR1_{23}$ biofilter at 1.21 mg TCE/L of air. Filled circle (●) represents experimental data (standard deviation shown), solid line (—) represents model prediction, and dotted line (· · · ·) represents model prediction with corrected biomass (20% less than the measured).

Model Assumptions and Effects

The assumption (1) of solid, inert, non-porous carriers is valid because most of the biofilm found was present outside the carriers and in the interstitial space (Sun and Wood, 1997). Assuming the solid carriers are homogenous in size with a uniform liquid/biofilm thickness around the carriers (assumption 2) was needed to estimate the parameter a (interfacial area of gas/liquid) for the calculation of the overall mass transfer coefficient for TCE and oxygen. Because the model showed there was no mass-transfer resistance from the gas to the liquid phase (compared to the biodegradation rate), the accuracy of parameter a is less critical. Images obtained from CSLM showed the structure and composition of the biofilm (live cells, dead cells, and void space); it consists of thick clumps of live and dead cells which were evenly distributed throughout the biofilm. Hence, the assumption (3) of no boundary separating the liquid and the biofilm is valid. The most important assumption (assumption 4) affecting the model was that the biomass concentration measured at the end was basically that present during

the experiments. The experiments lasted 1–13 d after TCE degradation, and the results of numerical simulation using the average biomass measured agreed well with the experimental data. However, quantifying the biomass concentration along the biofilter should improve the model predictions.

The Model and Its Implications

There are many advantages of immobilized cells on carriers, but the nature of immobilization can affect system kinetics. In many cases, immobilization of cells can result in mass-transfer limitations from the gas phase to the liquid phase (Karel et al., 1985). Comparing the relative magnitude of the film mass transfer and the biodegradation term of all the experimental runs (0.04 to 2.42 mg TCE/L), the maximum mass transfer term $[K_{L,TCE}\, a/\varepsilon(C^*_{l,TCE})]$ is 2000-fold greater than the maximum biodegradation term

$$[V_{max}XC^*_{l,TCE}/(K_{M,TCE} + C^*_{l,TCE})].$$

Because the immobilization of cells did not cause significant mass-transfer resistance from the gas to the liquid phase (compared to the biodegradation rate), TCE degradation was not limited by the availability of oxygen in the biofilms. Based on model simulations, for an inlet oxygen gas concentration of 272 mg/L (i.e., air), the minimum liquid oxygen concentration at the biofilter *outlet* ranged from 0.2 mg/L to 5.4 mg/L (hence, most regions had oxygen concentrations greater than 1.7 mg/L). Therefore, in some of the experiments the outlet regions of the biofilter had oxygen concentrations around the critical oxygen concentration (1.7 mg O_2/L) reported by Leahy et al. (1996) where a considerable loss of function by Tom was detected. However, the loss of Tom activity was not due to oxygen starvation in this study because effluent $PR1_{23}$ cells did not regain Tom activity overnight on Tom-indicating plates, after culturing in shake-flasks for three passages, or in the phenol-oxidation assay (Sun and Wood, 1997). As reported in the literature, most biofilm structures have microchannels formed by the extensive network of voids within the biofilm that facilitate the transport of nutrients and gases (de Beer et al., 1994; Massol-Deyá et al., 1995; Møller et al., 1996). These channels within the biofilm have been shown to increase the biological surface area significantly and provide as much as 50% of oxygen consumed by the biofilm (de Beer et al., 1994; Massol-Deyá et al., 1995). Thus, even with an increase in the oxygen concentration in the inlet gas stream (fivefold increase), improved TCE degradation was not predicted (less than 1%).

Changing the parameter values used in the model can facilitate understanding the significance of each term. Changes in the concentration of active biomass and transformation capacity (T_C) had the greatest improvements in predicted biofilter performance. Because TCE degradation depends on the available biomass, an increase in biomass concentration will lead to greater amount of biomass for TCE degradation and extend the biofilter operation. Figure 8 shows that a 10-fold increase in biomass leads to a significantly lower effluent TCE concentration (1.78 mg/L vs. 0.0 mg/L for a 10-fold increase in biomass after 1000 min of TCE addition).

A microorganism with high resistance to the toxic intermediates formed by TCE metabolism can degrade more TCE and prolong biofilter performance. Figure 8 shows that a 100-fold increase in T_C (Table III) leads to a 72% decrease in the effluent TCE concentration after 1000 min of TCE addition (1.78 mg/L vs. 0.49 mg/L for a 100-fold increase in T_C) and greater than a 95-fold increase in the breakthrough time (1580 min for control vs. 151,400 min for a 100-fold increase in T_C). Different microorganisms have been shown to have different levels of resistance to protein deactivation caused by TCE metabolism. Values for transformation capacity range from 0.031 mg of TCE/mg of cells [assuming 50% of total dried cell weight is cellular protein (Bailey and Ollis, 1986)] for a consortium of phenol oxidizers (Chang and Alvarez-Cohen, 1995), 0.04 to 0.06 mg TCE/mg cells for some methane oxidizers (Alvarez-Cohen and McCarty, 1991; Chang and Alvarez-Cohen, 1995; Chu and Alvarez-Cohen, 1996), 0.0079 mg TCE/mg protein for an ammonia-oxidizer (Hyman et al., 1995), and as high as 0.082 mg TCE/mg cells (assuming 50% of total dried cell weight is cellular protein) for phenol-amended cells (Shurtliff et al., 1996).

If *Methylosinus trichosporium* OB3b, which has a 28-fold higher V_{max} (0.067 mg TCE/min/mg protein) and $K_{M,TCE}$ (19 mg/L) (Oldenhuis et al., 1991; Oldenhuis et al., 1989), was used in the biofilter to degrade 2.42 mg TCE/L, it is predicted the *M. trichosporium* OB3b biofilter would degrade TCE initially at a higher efficiency than the $PR1_{23}$ biofilter [0.0 mg TCE/L for *M. trichosporium* OB3b vs. 0.6 mg TCE/L for $PR1_{23}$ in the effluent air after 100 min of TCE addition assuming T_C and active biomass are the same (Fig. 8)]. However, because enzyme deactivation is proportional to the TCE degradation rate [Eq. (5)], faster enzyme deactivation will result in earlier loss of enzyme activity; therefore, breakthrough occurs faster assuming new biomass does not express active TCE-degrading enzyme (breakthrough time of 600 min for *M. trichosporium* OB3b vs. 1600 min for $PR1_{23}$).

For $PR1_{23}$, if the volumetric air flow rate was decreased by 10-fold (0.01 L/min) while maintaining the same TCE concentration and active biomass concentration, the higher residence time of TCE in the biofilter would lead to a lower TCE concentration in the effluent stream [1.78 mg TCE/L for 0.1 L/min vs. 0.0 mg TCE/L for 0.01 L/min after 1000 min of TCE addition (Fig.8)]. Hence, the performance of the biofilter is extended because significantly less TCE is introduced.

The range of TCE concentrations found in drinking water wells is 600 to 14,000 parts per billion (0.6 to 14 mg TCE/L) (Council on Environmental Quality, 1981), and the maximum level of TCE allowed in drinking water is only 5 ppb (0.005 mg/L) (Steinberg and DeSesso, 1993). To size a biofilter for TCE degradation using the data in this report, it

is reasonable to assume the TCE concentration in the gas is in equilibrium with water at 0.6 mg TCE/L (0.24 mg/L in the gas phase). Hence, the estimated biofilter length necessary for degrading 99.5% of 0.24 mg TCE/L in 1 L air/min for a period of 50 d ranges from a minimum of 21 meters for the maximum biomass concentration of 18.0 mg/mL liquid (Table III) and a transformation capacity (T_C) of 0.204 mg TCE/mg protein to greater than 120 meters for the minimum biomass concentration of 4.2 mg/mL liquid and T_C of 0.065 mg TCE/mg protein.

CONCLUSIONS

Effective gas-phase TCE degradation and mineralization was shown using a fixed-film bioreactor with a pure culture (Sun and Wood, 1997). A mathematical model was developed for describing TCE degradation in a biofilter using *B. cepacia* $PR1_{23}$ which constitutively expresses a TCE-degrading enzyme. The numerical simulations agreed relatively well with the experimental data for abiotic and biotic controls as well as for four experiments at different TCE concentrations. Based on the simulation results, TCE degradation was not limited by the available oxygen and TCE in the biofilm (i.e., mass transfer resistance was insignificant relative to biodegradation). The most important parameters for improving the biofilter performance were determined to be the amount of active biomass for TCE degradation and the transformation capacity for TCE degradation.

Improvements such as higher maximum TCE degradation rates (V_{max}) or increasing the affinity of the biofilm toward TCE (decreasing $K_{M,TCE}$) should not enhance TCE removal in the biofilter as long as the new biomass formed does not produce active TCE-degrading enzyme. Inactivated Tom in the $PR1_{23}$ cells used here was not due to oxygen starvation or loss of reductant supply as the biofilter effluent cells did not recover Tom activity overnight on Tom-indicating plates or during the phenol oxidation assay (although they retained the *tom* genes). This suggests cyclic biofilter operation may be best to generate new biomass with Tom activity. The best microorganism for TCE degradation should have high TCE-degrading enzyme activity, high transformation capacity for TCE, and grow relatively rapidly.

We owe special thanks to Mr. M. J. Reagin and Professor M. S. Shields for providing the strains used for this study. We also thank Mr. Rolf Jaeger from the Jaeger Biotech Engineering, Inc., Costa Mesa, California for his generous gift of the SIRAN™ carriers. We also thank Youn Sim for his help in computer programming.

NOMENCLATURE

a	interfacial area of gas/liquid per a unit of reactor volume (1/cm)
A	cross-sectional area of biofilter (cm^2)
$C_{g,O2}$	O_2 concentration in gas phase (mg/L)
$C_{g,TCE}$	TCE concentration in gas phase (mg/L)
$C^*_{l,O2}$	liquid–phase O_2 concentration at the gas/liquid interface (mg/L)
$C^*_{l,TCE}$	liquid–phase TCE concentration at the gas/liquid interface (mg/L)
$C_{l,O2}$	O_2 concentration in liquid phase (mg/L)
$C_{l,TCE}$	TCE concentration in liquid phase (mg/L)
D_{AB}	gas-phase diffusivity (cm^2/min)
$D_{g,O2}$	axial dispersion coefficient of O_2 in gas phase (cm^2/min)
$D_{g,TCE}$	axial dispersion coefficient of TCE in gas phase (cm^2/min)
$D_{l,O2}$	axial dispersion coefficient of O_2 in liquid phase (cm^2/min)
$D_{l,TCE}$	axial dispersion coefficient of TCE in liquid phase (cm^2/min)
d_p	carrier diameter (cm)
H_{TCE}	Henry's constant for TCE (dimensionless)
H_{O2}	Henry's constant for O_2 (dimensionless)
$K_{L,O2}a$	overall volumetric liquid mass transfer coefficient for O_2 per volume of bed (1/min)
$K_{L,TCE}a$	overall volumetric liquid mass transfer coefficient for TCE per volume of bed (1/min)
$K_{M,O2}$	Michaelis constant for O_2 (mg/L)
$K_{M,TCE}$	Michaelis constant for TCE (mg/L)
Q_A	volumetric air flow rate (L/min)
Q_l	volumetric liquid nutrient flow rate (L/min)
t	time (min)
T_C	transformation capacity (mg TCE/mg protein)
v	interstitial air velocity (cm/min)
V_{max}	maximum TCE degradation rate (mg TCE/min/mg protein)
X	average concentration of active biomass (mg protein/L)
x	axial length of biofilter (cm)
Y_{resp}	O_2 consumption for background respiration (mgO_2/min mg protein)
Y_{O2}	O_2 consumption due to TCE degradation (mg O_2/mg TCE)
Re′	$\frac{Q_A d_p}{\nu A(1-\varepsilon_b)\gamma}$
Sc	$\frac{\nu}{D_{AB}}$
Sh′	$\frac{K_L d_p}{D_{AB}}\left(\frac{\varepsilon_b}{1-\varepsilon_b}\right)\frac{1}{\gamma}$

Greek Letters

γ	shape factor (external surface area divided by $\pi {d_p}^2$)
δ	biofilm thickness (cm)
ε	liquid hold-up volume around the SIRAN™ beads (cm^3 of liquid/cm^3 of bed)
ε_b	void fraction of packed bed ($\varepsilon + \theta$)
ν	kinematic viscosity (cm^2/min)
θ	bed porosity of the biofilter (cm^3 of gas/cm^3 of bed)

References

Alvarez-Cohen, L., McCarty, P. L. 1991. A cometabolic biotransformation model for halogenated aliphatic compounds exhibiting product toxicity. Environ. Sci. Technol. **25**: 1381–1387.

Alvarez-Cohen, L., McCarty, P. L. 1991. Product toxicity and cometabolic competitive inhibition modeling of chloroform and trichloroethylene transformation by methanotrophic resting cells. Appl. Environ. Microbiol. **57**: 1031–1037.

Bailey, J. E., Ollis, D. F. 1986. Biochemical engineering fundamentals. McGraw-Hill, New York.

Beyenal, H., Seker, S., Tanyolaç, A., Salih, B. 1997. Diffusion coefficients of phenol and oxygen in a biofilm of *Pseudomonas putida.* AIChE J. **43**: 243–250.

Chang, H.-L., Alvarez-Cohen, L. 1995. Model for the cometabolic biodegradation of chlorinated organics. Environ. Sci. Technol. **29**: 2357–2367.

Chang, H.-L., Alvarez-Cohen, L. 1995. Transformation capacities of chlo-

rinated organics by mixed cultures enriched on methane, propane, toluene, or phenol. Biotechnol. Bioeng. **45**: 440–449.

Chu, K.-H., Alvarez-Cohen, L. 1996. Trichloroethylene degradation by methane-oxidizing cultures grown with various nitrogen sources. Wat. Environ. Res. **68**: 76–82.

Council on Environmental Quality. 1981. Contamination of ground water by toxic organic chemicals. U.S. Government Printing Office, Washington, DC. GA 1.13:CED-81-66.

Coyle, C. G., Parkin, G. F., Gibson, D. T. 1993. Aerobic, phenol-induced TCE degradation in completely mixed, continuous-culture reactors. Biodegradation **4**: 59–69.

de Beer, D., Stoodley, P., Roe, F., Lewandowski, Z. 1994. Effects of biofilm structures on oxygen distribution and mass transport. Biotech. Bioeng. **43**: 1131–1138.

Dikshitulu, S., Baltzis, B. C., Lewandowski, G. A., Pavlou, S. 1993. Competition between two microbial populations in a sequencing fed-batch reactor: Theory, experimental verification, and implications for waste treatment applications. Biotech. Bioeng. **42**: 643–656.

Duncan, G. B., Counce, R. M., Donaldson, T. L. 1995. A model of a fixed-film trickle-filter bioreactor for TCE degradation. Sep. Sci. Technol. **30**: 1791–1805.

Ensley, B. D., Kurisko, P. R. 1994. A gas lift bioreactor for vapor-phase destruction of chlorinated organics. Appl. Environ. Microbiol. **60**: 285–290.

Fan, L.-S., Leyva-Ramos, R., Wisecarver, K. D., Zehner, B. J. 1990. Diffusion of phenol through a biofilm grown on activated carbon particles in a draft-tube three-phase fluidized-bed bioreactor. Biotech. Bioeng. **35**: 279–286.

Fogler, H. S. 1992. Elements of chemical reaction engineering, 2nd edition. Prentice-Hall, Englewood Cliffs, NJ.

Folsom, B. R., Chapman, P. J. 1991. Performance characterization of model bioreactor for the biodegradation of trichloroethylene by *Pseudomonas cepacia* G4. Appl. Environ. Microbiol. **57**: 1602–1608.

Folsom, B. R., Chapman, P. J., Pritchard, P. H. 1990. Phenol and trichloroethylene degradation by *Pseudomonas cepacia* G4: Kinetics and interactions between substrates. Appl. Environ. Microbiol. **56**: 1279–1285.

Hao, O. J., Chen, J. M., Davis, A. P., Al-Ghusain, I. A., Phull, K. K., Kim, M. H. 1991. Biological fixed-film systems. Research J. WPCF. **63**: 388–394.

Hecht, V., Brebbermann, D., Bremer, P., Deckwer, W.-D. 1995. Cometabolic degradation of trichloroethylene in a bubble column bioscrubber. Biotech. Bioeng. **47**: 461–469.

Hodge, D. S., Devinny, J. S. 1995. Modeling removal of air contaminants by biofiltration. J. Environ. Eng. **121**: 21–32.

Hyman, M., Russell, S. A., Ely, R. L., Williamson, K. J., Arp, D. J. 1995. Inhibition, inactivation, and recovery of ammonia-oxidizing activity in cometabolism of trichloroethylene by *Nitrosomonas europaea*. Appl. Environ. Microbiol. **61**: 1480–1487.

Jayaraman, A., Sun, A. K., Wood, T. K. 1998. Characterization of axenic *P. fragi* and *E. coli* biofilms that inhibit corrosion of SAE 1018 steel. J. Appl. Microbiol. in press.

Karel, S. F., Libicki, S. B., Robertson, C. R. 1985. The immobilization of whole cells: Engineering principles. Chem. Eng. Sci. **40**: 1321–1354.

Kirchner, K., Wagner, S., Rehm, H.-J. 1992. Exhaust gas purification using biocatalysts (fixed bacteria monocultures): The influence of biofilm diffusion rate (O_2) on the overall reaction rate. Appl. Microbiol. Biotech. **37**: 277–279.

Lackey, L. W., Phelps, T. J., Bienkowski, P. R., White, D. C. 1993. Biodegradation of chlorinated aliphatic hydrocarbon mixtures in a single-pass packed-bed reactor. Appl. Biochem. Biotechnol. **39**: 701–713.

Landa, A. S., Sipkema, M. E., Weijma, J., Beenackers A. A. C. M., Dolfing J., Janssen D. B. 1994. Cometabolic degradation of trichloroethylene by *Pseudomonas cepacia* G4 in a chemostat with toluene as the primary substrate. Appl. Environ. Microbiol. **60**: 3368–3374.

Leahy, J. G., Bryne, A. M., Olsen, R. H. 1996. Comparison of factors influencing trichloroethylene degradation by toluene-oxidizing bacteria. Appl. Environ. Microbiol. **62**: 825–833.

Mak, A. N. S., Koning, C. A. J., Hamersma, P. J., Fortuin, J. M. H. 1991. Axial dispersion in single-phase flow in a pulsed packed column containing structured packing. Chem. Eng. Sci. **46**: 819–826.

Massol-Deyá, A. A., Whallon, J., Hickey, R. F., Tiedje, J. M. 1995. Channel structures in aerobic biofilms of fixed-film reactors treating contaminated groundwater. Appl. Environ. Microbiol. **61**: 769–777.

McFarland, M. J., Vogel, C. M., Spain, J. C. 1992. Methanotrophic cometabolism of trichloroethylene (TCE) in a two stage bioreactor system. Wat. Res. **26**: 259–265.

Møller, S., Pedersen, A. R., Poulsen, L. K., Arvin, E., Molin, S. 1996. Activity and three-dimensional distribution of toluene-degrading *Pseudomonas putida* in a multispecies biofilm assessed by quantitative in situ hybridization and scanning confocal laser microscopy. Appl. Environ. Microbiol. **62**: 4632–4640.

Nelson, M. J. K., Montgomery, S. O., O'Neil, E. J., Pritchard, P. H. 1986. Aerobic metabolism of trichloroethylene by a bacterial isolate. Appl. Environ. Microbiol. **52**: 383–384.

Oldenhuis, R., Oedzes, J. Y., Waarde, J. J. V. D., Janssen, D. B. 1991. Kinetics of chlorinated hydrocarbon degradation by *Methylosinus trichosporium* OB3b and toxicity of trichloroethylene. Appl. Environ. Microbiol. **57**: 7–14.

Oldenhuis, R., Vink, R. L. J. M., Janssen, D. B., Witholt, B. 1989. Degradation of chlorinated aliphatic hydrocarbons by *Methylosinus trichosporium* OB3b expressing soluble methane monooxygenase. Appl. Environ. Microbiol. **55**: 2819–2826.

Ottengraf, S. P. P., Van Den Oever, A. H. C. 1983. Kinetics of organic compound removal from waste gases with a biological filter. Biotech. Bioeng. **25**: 3089–3102.

Parvatiyar, M. G., Govind, R., Bishop, D. F. 1996. Treatment of trichloroethylene (TCE) in a membrane biofilter. Biotech. Bioeng. **50**: 57–64.

Phelps, T. J., Niedzielski, J. J., Schram, R. M., Herbes, S. E., White, D. C. 1990. Biodegradation of trichloroethylene in continuous-recycle expanded-bed bioreactors. Appl. Environ. Microbiol. **56**: 1702–1709.

Shareefdeen, Z., Baltzis, B. C., Oh, Y. S., Bartha, R. 1993. Biofiltration of methanol vapor. Biotech. Bioeng. **41**: 512–524.

Shields, M. S., Montgomery, S. O., Cuskey, S. M., Chapman, P. J., Pritchard, P. H. 1991. Mutants of *Pseudomonas cepacia* G4 defective in catabolism of aromatic compounds and trichloroethylene. Appl. Environ. Microbiol. **57**: 1935–1941.

Shields, M. S., Reagin, M. J. 1992. Selection of a *Pseudomonas cepacia* strain constitutive for the degradation of trichloroethylene. Appl. Environ. Microbiol. **58**: 3977–3983.

Shields, M. S., Reagin, M. J., Gerger, R. R., Somerville, C., Schaubhut, R., Campbell, R., Hu-Primmer, J. 1994. Constitutive degradation of trichloroethylene by an altered bacterium in a gas-phase bioreactor, p. 50–65. In: R. E. Hinchee, A. Leeson, L. Semprini, and S. K. Ong (eds.), Bioremediation of chlorinated and polycyclic aromatic hydrocarbon compounds. Lewis Publishers, Boca Raton, FL.

Shurtliff, M. M., Parkin, G. F., Weathers, L. J., Gibson, D. T. 1996. Biotransformation of trichloroethylene by a phenol-induced mixed culture. J. Environ. Eng. **122**: 581–589.

Singleton, P., Sainsbury, D. 1988. Dictionary of microbiology and molecular biology, 2nd edition. Wiley, New York.

Steinberg, A. D., DeSesso, J. M. 1993. Have animal data been used inappropriately to estimate risks to humans from environmental trichloroethylene? Regul. Toxicol. Pharmacol. **18**: 137–153.

Strand, S. E., Wodrich, J. V., Stensel, D. H. 1991. Biodegradation of chlorinated solvents in a sparged, methanotrophic biofilm reactor. Res. J. WPCF. **63**: 859–866.

Sun, A. K., Wood, T. K. 1996. Evaluation of trichloroethylene degradation and mineralization by pseudomonads and *Methylosinus trichosporium* OB3b. Appl. Microbiol. Biotech. **45**: 248–256.

Sun, A. K., Wood, T. K. 1997. Trichloroethylene mineralization in a fixed-film bioreactor using a pure culture expressing constitutively toluene *ortho*-monooxygenase. Biotech. Bioeng. **55**: 674–685.

Taylor, R. T., Hanna, M. L., Shah, N. N., Shonnard, D. R. 1993. In situ bioremediation of trichloroethylene-contaminated water by a resting-cell methanotrophic microbial filter. Hydrol. Sci. J. **38**: 323–342.

Utgikar, V., Govind, R., Shan, Y., Safferman, S., Brenner, R. C. 1991. Biodegradation of volatile organic chemicals in a biofilter, p. 233–260. In: D. W. Tedder and F. G. Pohland (eds.), Emerging technologies in hazardous waste management II. American Chemical Society, Washington, DC.

Wackett, L. P., Gibson, D. T. 1988. Degradation of trichloroethylene by toluene dioxygenase in whole-cell studies with *Pseudomonas putida* Fl. Appl. Environ. Microbiol. **54**: 1703–1708.

Wackett, L. P., Householder, S. R. 1989. Toxicity of trichloroethylene to *Pseudomonas putida* F1 is mediated by toluene dioxygenase. Appl. Environ. Microbiol. **55**: 2723–2725.

Wang, K.-W., Tsangaris, D. M., Baltzis, B. C., Lewandowski, G. A. 1996. Biodegradation of mixed wastes in continuously operated cyclic reactors. Appl. Biochem. Biotechnol. **57/58**: 803–815.

Wankat, P. C. 1990. Rate-controlled separations. Elsevier London.

Westerterp, K. R., Van Swaaij, W. P. M., Beenackers, A. A. C. M. 1984. Chemical reactor design and operation. Wiley, New York.

Wilcox, D. W., Autenrieth, R. L., Bonner, J. S. 1995. Propane-induced biodegradation of vapor phase trichloroethylene. Biotechnol. Bioeng. **46**: 333–342.

Zilli, M., Converti, A., Lodi, A., Del Borghi, M., Ferraiolo, G. 1993. Phenol removal from waste gases with a biological filter by *Pseudomonas putida.* Biotechnol. Bioeng. **41**: 693–699.

Zylstra, G. J., Wackett, L. P., Gibson, D. T. 1989. Trichloroethylene degradation by *Escherichia coli* containing the cloned *Pseudomonas putida* F1 toluene dioxygenase genes. Appl. Environ. Microbiol. **55**: 3162–3166.